STUDY OF THERMAL STABILITY AND QUENCH PROCESS OF HTS DIPOLE

V. Zubko, I. Bogdanov, S. Kozub, P, Shcherbakov, L.Tkachenko, Institute for High Energy Physics (IHEP), Protvino, Moscow region, Russia, 142281

INTRODUCTION

Analysis of thermal stability of low temperature superconducting (LTS) conductors is based on the "equal area" criterion [1]. This criterion known as a necessary and sufficient condition in order to a superconductor at operating current and magnetic field can not evolve towards a resistive state after an accidental local overheating. The critical current for LTS conductor determines its current-carrying capacity. Thermal stability and transition into the normal condition of high temperature superconducting (HTS) conductors strongly differ from similar processes in LTS conductors. The main difference is the transition to the normal condition of HTS conductors occurs not as stepwise change, but gradually, in some intervals of temperature, current and magnetic field (smooth transition). A precise border between a normal phase and superconducting state in a HTS conductor does not exist due to smooth transition and a speed of normal phase distribution cannot be defined. The current, determining border of instability in HTS conductor, called as a thermal quench current I_q. The analytical model for analysis of thermal stability, transition to a normal condition and definitions I_q for HTS conductors are described in [2]. The thermal quench current I_q limits the operating current in real HTS conductors, so I_q can be considered as usual critical current in LTS conductors. The value of I_q can be much higher than critical current I_c (determined by 1 μV/cm criteria) in HTS conductors.

The analytical model, described in [2], is inapplicable for HTS coils, which are in non-uniform magnetic field. Moreover, dependence of a critical current on a magnetic field of HTS tapes is strongly anisotropic [3]. Measurements of voltage-current characteristics (VAC) of HTS tapes, carried out in IHEP [4], confirmed, that they also have anisotropy (anisotropy of VAC).

Developed in IHEP computer code HQUEN is based on the numerical method, allowing one to calculate stability and transition into a normal condition of HTS coils, taking into account smooth transition and anisotropy of VAC of HTS tapes. Analysis of these processes has been made with help of this code for HTS dipole, developed and produced in IHEP [4].

MAGNET DESIGN

HTS tape with 61 Bi2223 ceramic filaments into silver matrix was used as a current carrying element of the dipole. The filling factor of the conductor over ceramic filaments is 30 %. The tape dimensions are 3.8 mm × 0.25 mm. A “Racetrack” type coil is used in the magnet. Each half of the coil was wound on a stainless steel frame and was consisted of 356 turns stacked in 20 layers. Each turn was insulated from adjacent turn by means of installation of polyester filament. 40 μm thick Kapton film was used as the insulation between layers. The length of straight part of the coil is 400 mm and it is equal to the length of an iron yoke. The total length of the coil is 590 mm. The original iron shape allows one to minimize magnetic field in the coil. A nominal magnetic field is 1 T. An operating current I_{op} is 24 A. The HTS dipole was immersed into liquid nitrogen bath. Dipole tests were carried out at 77 K at atmospheric pressure, and at 65 K with a vapor pumping. The general view of the magnet, cross-section in the first quadrant and part of coil are presented in Fig. 1. The detailed description of the HTS dipole design is given in [4].

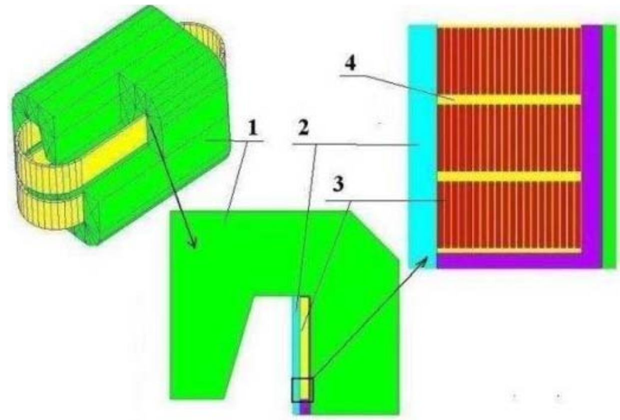

Figure 1. General view, cross-section in the first quadrant and part of the dipole: 1 - iron yoke; 2 - stainless steel frame; 3 - HTS -coil; 4 - epoxy compound.

COMPUTATIONAL MODEL

The transition characteristic of HTS tape is assumed to be

$$E = E_c \left(\frac{J}{J_c(T,B,\theta)} \right)^{n(T,B,\theta)}, \qquad (1)$$

where E_c = 1 μV/cm, J_c is the critical current determined by 1 μV/cm criteria, n is the index number of superconductor. J_c and n depend on temperature T, magnetic field B and angle θ between vector of magnetic flux density and broad surface of the tape. Dependences $J_c = J_c(\theta)$ and $n = n(\theta)$ allow one to take into account VAC anisotropy of HTS tapes.

For simulations of transition in a normal condition of HTS coil, the computer code solves the thermal conductivity equation by the finite difference method:

$$C(T)\frac{\partial T}{\partial t} = \nabla(\lambda(T)\nabla T) + Q\,, \qquad (2)$$

where C and λ are the effective volumetric specific heat and the thermal conductivity in the coil and in other materials of the dipole. Boundary conditions are determined by heat transfer into nitrogen (free-convection or heat transfer into boiling nitrogen).

Heat generation in the HTS composite tape is $Q = E \times J$. In composite superconductor the longitudinal electric field can be defended separately, $E = \rho_m(T) \times J_m$ in matrix of HTS tapes, and $E = \rho_s(T,J,B,\theta) \times J_s$ in superconducting filaments, where $\rho_m(T)$ is the specific resistivity of matrix, $\rho_s(T,J,B,\theta)$ is the non-linear specific resistivity of HTS tape, J_m, J_s are the current densities in matrix and superconducting filaments correspondingly. Taking into account (1), the specific resistivity of HTS tape can be approximated as

$$\rho_s(T,J,B,\theta) = E_c \frac{J^{\,n(T,B,\theta)-1}}{J_c(T,B,\theta)^{n(T,B,\theta)}}\,. \qquad (3)$$

An implicit equation set is used for calculation of current density J_m, J_s:

$$J_m S_m = I(t) - J_s S_s\,,$$
$$J_s S_s\left(\rho_m(T) + \frac{S_m}{S_s}\rho_s(T,J,B,\theta)\right) = \rho_m(T) I \qquad (4)$$

Here $I(t)$ is the total current in the turn, t is time, S_m and S_s are the cross sectional areas of matrix and superconducting filaments. Non-linear set of equations (4) is solved by using iterative algorithm for each spatial element of the coil and as function of time.

The code MULTIC [5] is used for determination of magnetic field components (with taking into account real magnetic permeability in iron yoke) at stage of solution of (4) for a finding $J_c(T,B,\theta)$ and $n(T,B,\theta)$. The output file with calculated magnetic flux density $|B(x,y,t)|$ and its components $B_x(x,y,t)$ and $B_y(x,y,t)$ is as input file for HQUEN. An angle between vector of magnetic flux density and broad surface of the tape for each spatial element is determined by $\theta(x,y) = \arctan\left(\frac{B_x(x,y)}{B_y(x,y)}\right)$.

HTS TAPE PROPERTIES

Three short samples were cut from the pieces of tape, which was used for coil manufacturing. Fig. 2 presents distribution of normalized critical current $I_c(T = 77\,K,B,\theta)/I_c(T = 77\,K,B = 0,\theta = 0)$.

Critical currents $I_c(T = 77\,K,B = 0,\theta = 0)$ of the three HTS tapes, determined by 1 µV/cm criteria, was about 20 A [4]. Dependences of the normalized critical current $I_c(T = 77\,K,B,\theta)/I_c(T = 77\,K,B = 0,\theta = 0)$ as well as of $n(T = 77\,K,B,\theta)$ are almost the same for three HTS tapes with spread about 10 %.

Fig. 3 presents $n(T = 77\,K,B,\theta)$ for measured HTS tapes.

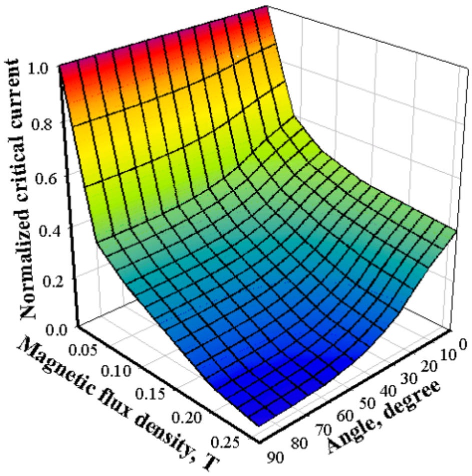

Figure 2. The normalized critical current of HTS tapes as a function of magnitude and orientation of magnetic field.

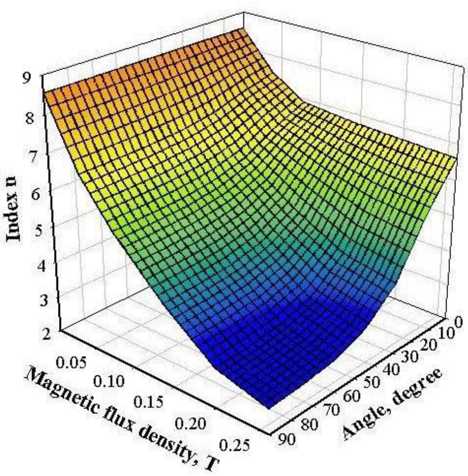

Figure 3. The index number n of HTS tapes as a function of magnitude and orientation magnetic field.

CALCULATED AND TESTED RESULTS

Fig. 4 presents distributions of magnetic field $|B|$, B_x, B_y, components and angle θ in the first quadrant of the coil at operating current I_{op}.

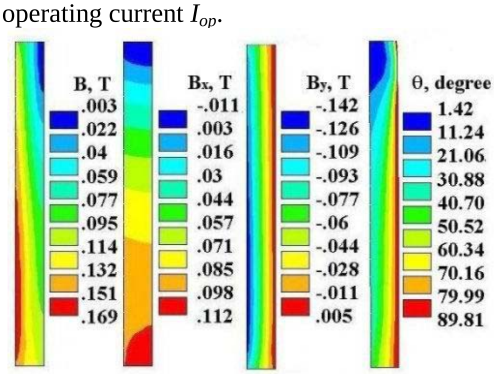

Figure 4. Distribution of magnetic field $|B|$, B_x, B_y components, angle θ in the coil of HTS dipole.

The maximal magnetic field $|B|$ is found in the first layer whereas maximal angle θ is found in the last layer.

As dependences of I_c as well as of n for three HTS tapes are almost the same, an assumption was made in numerical calculation, that the critical current I_c is constant along the whole length of HTS tape in the coil.

Fig. 5 shows the calculated results of thermal quench current I_q and minimal critical current in the coil I_{Cmin} at $I_{op} = I_q$ versus $I_c(T = 77\ K, B = 0, \theta = 0)$ of HTS tape. To guarantee a stability of the HTS dipole, the operating current of 24 A must be higher then thermal quench current I_q. Fig. 5 shows that the critical current $I_c(T = 77\ K, B = 0, \theta = 0)$ in HTS tape must be larger 22 A.

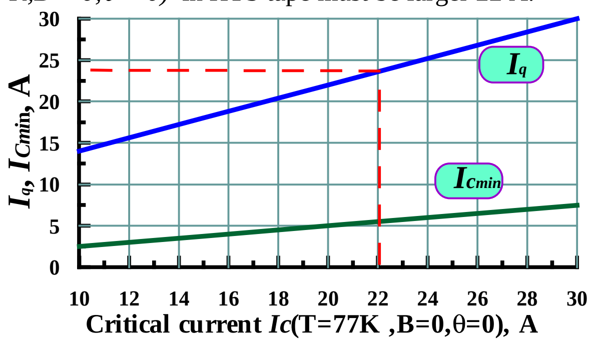

Figure 5. Dependence of thermal quench current I_q and minimal critical current in the coil I_{Cmin} at $I_{op} = I_q$ versus $I_c(T = 77\ K, B = 0, \theta = 0)$ of HTS tape.

Distributions of critical current (1 µV/cm) and temperature in the coil are shown in Fig. 6 at the operating current, when $I_c(T = 77\ K, B = 0, \theta = 0) = 22$ A of HTS tape. In this case operating current is close to I_q.

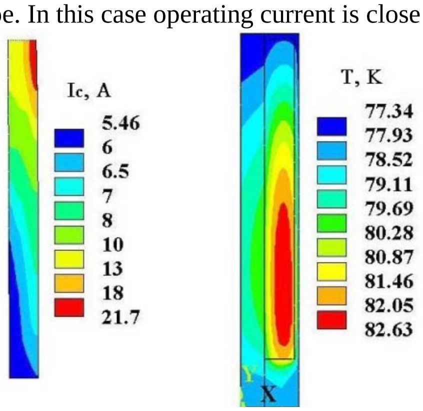

Figure 6. Distributions of critical current and temperature in cross-section of the coil at operating current (77 K).

One can see the values of the operating current exceed critical current almost in the whole of the coil. I_{Cmin} = 5.46 A and the maximal difference between the operating current and the critical current in the coil is about 18 A. However the HTS dipole does not transit in the normal state. Smooth transition in HTS tape is determined by the index number of superconductor, which lies in the region of $3 < n < 8$ for given current carrying element. So large difference between operating current and minimal critical current in the coil is explained by low value of n as well as by good cooling of the coil. A stability of HTS magnets is lost because of increase in temperature, caused by heat generation, distributed over the whole coil but it is not due to the propagation of a local normal zone. In addition voltage drop for the whole coil is about 5 V and maximal heating of the coil is about 5 K at operating current close to I_q.

Tests showed that current carrying capability of the HTS tape is decreased during magnet manufacturing. The measured values of thermal quench currents I_q were 13 A and 22 A for temperatures of nitrogen 77 K and 65 K, correspondingly. Low I_q points out on critical current degradation of HTS tape in comparison with critical current of the short samples. One can see from Fig. 5 the values of $I_c(T = 77\ K, B = 0, \theta = 0)$ of HTS tape after magnet assembly are about 10 A and 20 A at temperature of nitrogen 77 K and 65 K correspondingly.

Numerical calculations of transition in a normal condition of the HTS dipole have been made for $I_c(T = 77\ K, B = 0, \theta = 0)$ of HTS tape, equal to 10 A and 20 A. Fig. 7 shows voltage-current characteristics of the HTS dipole at different temperature, where the voltage drop was calculated and measured for the whole coil.

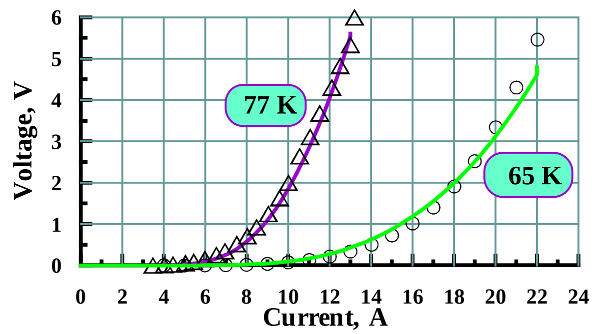

Figure 7. Calculated (solid line) and measured VAC of the HTS dipole at different temperature.

CONCLUSION

The numerical model for stability study of HTS magnet has been developed. This model takes into account the characteristic features of HTS tape (smooth transition and anisotropy of VAC HTS tapes). It has been shown on the basis of numerical simulations that the HTS dipole has thermal quench current I_q much higher than minimal critical current in coil I_{Cmin}, which is explained by low enough value of the index number in the HTS tape and by good cooling of the coil. There are good agreement between calculations and experimental results.

REFERENCES

[1] Wilson M.N. "Superconducting magnets," Claredon Press, Oxford, 1983.

[2] Rakhmanov A.L. et al. "Universal Scaling Law for Quench Development in HTSC Devices," Cryogenics, 2000, vol. 40, no. 1.

[3] Kovach P. et al. "Influence of the Winding Geometry on the Critical Currents and Magnetic Fields of Cylindrical Coils Made of Bi(2223)Ag Anisotropic Tapes," IEEE Trans. on Applied Superconductivity, vol. 10, no. 1, Mar. 2000, pp. 478-481.

[4] Ageev A.I., et al. "Test results of HTS dipole," IEEE Trans. on Applied Superconductivity, vol. 12, no. 1, Mar. 2002, pp. 125-128.

[5] Tkachenko L.M. "Code Package MULTIC for Calculation of Magnetic Field with an Arbitrary Configuration," IHEP preprint 92-28, 1992, 48 pp